Original Article

Functional neuroimaging of responses to multiple sensory stimulations in newborns with perinatal asphyxia

Carla R. Pinto[1,2,3], João V. Duarte[3,4], Alexandra Dinis[1], Isabel C. Duarte[3,4], João Castelhano[3,4], Joana Pinto[5], Guiomar Oliveira[2,3,6], Miguel Castelo-Branco[3,4]

[1]Pediatric Intensive Care Unit, Pediatric Hospital, Coimbra Hospital and University Centre, Coimbra, Portugal; [2]University Clinic of Pediatrics, Faculty of Medicine, University of Coimbra, Coimbra, Portugal; [3]Coimbra Institute for Biomedical Imaging and Translational Research (CIBIT) and Institute of Nuclear Sciences Applied to Health (ICNAS), University of Coimbra, Coimbra, Portugal; [4]Faculty of Medicine, University of Coimbra, Coimbra, Portugal; [5]Neuroradiology Unit, Medical Imaging Department, Coimbra Hospital and University Centre, Coimbra, Portugal; [6]Child Developmental Center, Research and Clinical Training Center, Pediatric Hospital, Coimbra Hospital and University Centre, Coimbra, Portugal

Contributions: (I) Conception and design: CR Pinto, A Dinis, IC Duarte, J Castelhano, G Oliveira, M Castelo-Branco; (II) Administrative support: CR Pinto, JV Duarte; (III) Provision of study materials or patients: CR Pinto, A Dinis; (IV) Collection and assembly of data: CR Pinto, JV Duarte, A Dinis, IC Duarte, J Castelhano, J Pinto; (V) Data analysis and interpretation: CR Pinto, JV Duarte, IC Duarte, J Castelhano, J Pinto; (VI) Manuscript writing: All authors; (VII) Final approval of manuscript: All authors.

Correspondence to: Carla R. Pinto, MD. Pediatric Intensive Care Unit, Pediatric Hospital, Coimbra Hospital and University Centre, Afonso Romão Avenue, 3000-602 Coimbra, Portugal; University Clinic of Pediatrics, Faculty of Medicine, University of Coimbra, Coimbra, Portugal; Coimbra Institute for Biomedical Imaging and Translational Research (CIBIT) and Institute of Nuclear Sciences Applied to Health (ICNAS), University of Coimbra, Coimbra, Portugal. Email: carla.regina.pinto@gmail.com; carla.pinto@chuc.min-saude.pt.

Background: Functional neuroimaging can provide pathophysiological information in perinatal asphyxia (PA). However, fundamental unresolved questions remain related to the influence of neurovascular coupling (NVC) maturation on functional responses in early development. We aimed to probe the feasibility and compare the responses to multiple sensory stimulations in newborns with PA using functional magnetic resonance imaging (fMRI) and functional near-infrared spectroscopy (fNIRS).

Methods: Responses to visual, auditory, and sensorimotor passive stimulation were measured with fMRI and fNIRS and compared in 18 term newborns with PA and six controls.

Results: Most newborns exhibited a positive fMRI response during visual and sensorimotor stimulation, higher in the sensorimotor. An asymmetric pattern (negative in the left hemisphere) was observed in auditory stimulation. The fNIRS response most resembling the adult pattern (positive) in PA occurred during auditory stimulation, in which oxyhemoglobin (HbO) increased, and deoxyhemoglobin (HbR) decreased. Significative differences were found in the HbO and HbR profiles in newborns with PA compared to the controls, more evident in auditory stimulation. Positive correlations between the fMRI BOLD signal and at least one fNIRS channel (HbO) in all stimuli in newborns with PA were identified: the strongest was in the auditory (r=0.704) and the weakest in the sensorimotor (r=0.544); in more fNIRS channels, in the visual.

Conclusions: Both techniques are feasible physiological assessment tools, suggesting a distinctive level of maturation in sensory and motor areas. Differences in fNIRS profiles in newborns with PA and controls and the fMRI-fNIRS relationship observed can encourage the fNIRS as a clinically emergent valuable tool.

Keywords: Newborn; functional magnetic resonance imaging (fMRI); functional near-infrared spectroscopy (fNIRS); perinatal asphyxia (PA); multiple sensory stimulations

Submitted Mar 03, 2023. Accepted for publication Jul 21, 2023. Published online Sep 11, 2023.
doi: 10.21037/tp-23-135
View this article at: https://dx.doi.org/10.21037/tp-23-135

Introduction

Despite perinatal care improvement, including therapeutic hypothermia, hypoxic-ischemic encephalopathy (HIE) due to perinatal asphyxia (PA) remains a recognized cause of long-term neurodevelopmental disability (1,2). Conventional magnetic resonance imaging (MRI) and spectroscopy are considered good predictors of outcome (3,4). Nevertheless, this happens only in a binary manner, without the capacity to discriminate either long-term neurodevelopmental disorders or specific impairment of functional/cognitive domains. New methods to assess cerebral function are required to improve clinical decision-making (5-7). Functional MRI (fMRI) has become the gold standard for functional imaging of the human brain, being safely used on healthy and brain-injured newborns (5,8). It provides high spatial resolution and allows the probing of brain function in different domains, using different sensory stimulation paradigms (5,7). Cognitive neuroscientists have been increasingly using another promising tool, functional near-infrared spectroscopy (fNIRS), which, such as fMRI, indirectly detects neural activity through variations in blood oxygenation. fNIRS has the advantage of portability and the possibility of being applied in a naturalistic environment, in children of any age, due to its lower susceptibility to movement artifacts (6,9).

Highlight box

Key findings

- Polarized responses in both techniques during multiple sensory stimulations, less evident in sensorimotor.
- A significant positive correlation between functional magnetic resonance imaging (fMRI) and functional near-infrared spectroscopy (fNIRS) signals in all stimuli in newborns with perinatal asphyxia (PA).

What is known and what is new?

- Functional neuroimaging can provide novel information in PA. However, central unanswered questions remain related to the hemodynamic response model in neural activity in newborns.
- The responses observed support the hypothesis of different levels of neurovascular coupling maturation in distinct cortical regions, higher in sensorimotor. A relationship between fMRI and fNIRS was established.

What is the implication, and what should change now?

- This study reinforces the need to determine a personalized hemodynamic response function for this high-risk population. The observed fMRI-fNIRS relationship may potentiate to setup of fNIRS as a surrogate marker of fMRI in newborns with PA, optimizing its clinical bedside use.

Furthermore, while fMRI can detect changes in relative oxy/deoxyhemoglobin [blood-oxygen-level-dependent (BOLD) contrast], fNIRS can differentiate oxyhemoglobin (HbO) and deoxyhemoglobin (HbR), providing additional hemodynamic and oxygenation information. However, fNIRS has a lower spatial resolution and a limited ability to assess anatomy (6,7). Despite its potential, an important methodological aspect related to these techniques in the developing brain, still poorly clarified, is the hemodynamic response model to neural activity (7,10). In adults, an increase in local cerebral blood flow (CBF) following neural activity during stimulation underlies the positive BOLD fMRI signal and the increase in HbO in fNIRS trials (7,10). Nevertheless, functional imaging studies of newborns report variable hemodynamic response patterns concerning positive and negative modulations (5,6,8), which can be partially explained by physiological mechanisms (11).

A direct comparison of the two techniques in the same newborn cohort is lacking, allowing for fully characterizing the hemodynamic response in the developing brain and potentially bringing new insights into the current use of fNIRS as a useful clinical tool at the bedside.

Thus, the main aims of this study were to probe the feasibility and to establish a relationship between two distinct functional neuroimaging modalities signals in assessing multiple functional systems (visual, auditory, and sensorimotor). We hypothesize that there is a correlation between fNIRS and fMRI signals in each stimulus in newborns with PA. We present this article in accordance with the MDAR reporting checklist (available at https://tp.amegroups.com/article/view/10.21037/tp-23-135/rc).

Methods

Participants

All newborns, admitted to a tertiary pediatric intensive care unit (PICU) during the study period (April 2016 to March 2017), were recruited with the following eligibility criteria: born at or after 36 gestational weeks with PA defined according to the American College of Obstetricians and Gynaecologists' Task Force on Neonatal Encephalopathy, 2014 criteria (12). Exclusion criteria were major congenital malformation or chromosomal anomaly, according to clinical judgement, inherited errors of metabolism or stroke. Twenty newborns with PA comprised eligibility criteria; however, two were excluded due to death on the fifth day of age associated with adverse prognosis and redirecting of

care and inherited inborn error of metabolism.

A convenience control group was also enrolled, composed of six newborns admitted to the PICU without neurologic diseases, with a normal cerebral ultrasound and neurologic exam, with the following diagnosis [N]: sepsis and bacteremia without meningitis [2], Hirschsprung disease [1], congenital diaphragmatic hernia [1], intestinal atresia with volvulus [1], and cloacal malformation [1].

fMRI data acquisition was possible in all newborns with PA and in one control, due to denied parental consent in the remaining controls. fNIRS data were acquired in all participants. Newborns with PA performed MRI scanning at a median of 12.5 (IQR, 10–14.3) days of age, and fNIRS acquisitions with 4.5 (IQR, 2.9–9.3) hours difference. fNIRS acquisition in the control group was performed at a median of 11 (IQR, 10–14.3) days. fMRI and fNIRS were acquired on the 15th day, with an interval of 2.5 hours, in one control newborn. Functional imaging was performed during a period of hemodynamic and respiratory stability. A description of the demographic and clinical data of participants is presented in *Table 1*. All procedures were carried out in accordance with the Declaration of Helsinki (as revised in 2013). The study was approved by the Ethics Committee of the Faculdade de Medicina da Universidade de Coimbra, Portugal (Reference CE-029-2014). Informed written consent was obtained from parents of all participants after a full verbal and written explanation of the study.

Classification of the HIE grade on admission and the amplitude integrated electroencephalography worst background pattern at 48 to 72 hours of age was performed according to the Modified Sarnat Score (13) and Hellström-Westas (14), respectively.

Paradigm

Passive visual, auditory, and sensorimotor stimulation were performed in separate runs with an optimized block design paradigm (15), with the same protocols for acquisition of fMRI and fNIRS. Visual stimuli were presented on an MR compatible screen and delivered through a mirror fastened to the head coil (fMRI), and the onset of stimulation/baseline blocks were synchronized with fMRI volumes or in a standard computer screen positioned at 30 cm from the participants' eyes (fNIRS). A checkerboard was presented in 13 blocks of 20 s, flashing at frequencies of 1 to 4 Hz, interleaved with 14 baseline blocks (black screen) of 12 s (8). The room was dark during visual stimulation. For the auditory stimulus, 16 blocks of 14 s comprised a 20–80 dB tone (centered at a frequency of 1.3 kHz, modulated over a range of ±1 kHz at a rate of 8 Hz), interleaved with 16 baseline blocks (no sound) of 14 s, were delivered through MRI compatible headphones incorporated with standard neonatal ear shields (fMRI) or a computer (fNIRS) in a silent environment (16). For sensorimotor stimulation, 10 blocks of 14 s with bilateral forearm extension/flexion movements (frequency of ~1 Hz) were manually performed by a physician positioned inside the scanner gantry (fMRI) or next to the newborn (fNIRS) (17), and interleaved with 11 baseline blocks (no movement) of 14 s. A scheme of each stimulation task is presented in *Figure 1*.

MRI data acquisition

Structural and functional MRI data were acquired in the same session using a Siemens 3T TIM Trio scanner (Siemens AG, Healthcare, Erlangen, Germany), with a standard 20-channel head coil. To minimize head motion during the imaging session, foam cushions and sedation with intravenous midazolam or propofol were used. The MRI protocol included T1-weighted MPRAGE (0.83 mm isotropic voxel, 160 slices, TR/TE =2,300/3.5 ms) and T2-weighted turbo spin echo SPACE (0.83 mm isotropic voxel, 160 slices, TR/TE =3,200/443 ms) structural scans, diffusion weighted imaging (DWI), and T2*-weighted pulse sequences sensitive to BOLD contrast [TR/TE =2,080/31 ms, voxel size =2×2×2 mm^3, 29 axial slices (no gap), FOV =256×256 mm^2, FA =90º] with whole-brain coverage. Continuous monitoring (heart rate, peripheral oxygen saturation and temperature) of the newborns inside the scanner was provided by an intensive care pediatrician and nurse. Two expert neuroradiologists characterized and classified the HIE brain injury by the Weeke score, using T1-weighted, T2-weighted and DWI sequences (18).

fMRI data preprocessing

Data preprocessing was performed with BrainVoyager v21.2 (Brain Innovation, Maastricht, The Netherlands) and the FMRIB Software Library (FSL) v4.1.8 and included: intra-run realignment and motion correction, using rigid transformations (with MCFLIRT); motion scrubbing, by marking pairs of adjacent volumes with >0.5 mm of total translation or 0.5° of total rotation between them as motion "spikes" (19); slice timing correction; linear trends removal; and temporal high-pass filtering (5 cycles per run). Structural data were skull-stripped, corrected for

Table 1 Demographic and clinical data of the study participants

Demographic and clinical variables	Newborns with PA, N=18	Controls, N=6
Gestational age, weeks	39.5 (37.8 to 40)	39 (37.8 to 40)
Birth weight, grams	3,230 (2,803 to 3,540)	3,628 (2,679 to 4,290)
Sex, male	14	3
APGAR score 5´	6 (5 to 6)	10 (9 to 10)
APGAR score 10´	7 (6 to 8)	10 (10 to 10)
Blood pH 1st h of age	7.02 (6.9 to 7.06)	
Base excess 1st h of age, mmol/L	–17.8 (–21.1 to –14)	
Lactate on admission, mmol/L	15.2 (13 to 16)	
Grade of HIE on admission		
Mild	2	
Moderate	11	
Severe	5	
aEEG at 48 to 72 h of age		
Continuous	5	
Discontinuous	9	
Burst suppression	2	
Low voltage	1	
Inactive, flat	0	
Therapeutic hypothermia	16	
Mechanical ventilation	17	
Sedation	17	
Inotropes	15	
Anticonvulsants	7	
MRI		
Total score	2 (1 to 6.75)	
Deep grey matter subscore	0 (0 to 1.5)	
Cerebral white matter/cortex subscore	0 (0 to 5.25)	

Variables are expressed as median and interquartile range or absolute number, when appropriate. PA, perinatal asphyxia; N, total number; aEEG, amplitude integrated electroencephalography (worst background pattern); HIE, hypoxic-ischemic encephalopathy; MRI, magnetic resonance imaging.

inhomogeneities of signal intensity, and co-registered with functional scans. Slight spatial smoothing (full width half maximum kernel with 3 mm) was applied to functional data.

fMRI data analysis

The BOLD response to visual, auditory, or sensorimotor stimulation was estimated using a whole-brain voxel-wise general linear model (GLM). Regressors for each stimulation condition were defined as boxcar functions convolved with a term infant-specific two-gamma hemodynamic response function (HRF) (20). To reduce multiple comparison bias, the authors manually selected only voxels exhibiting BOLD signal increases with P<0.05

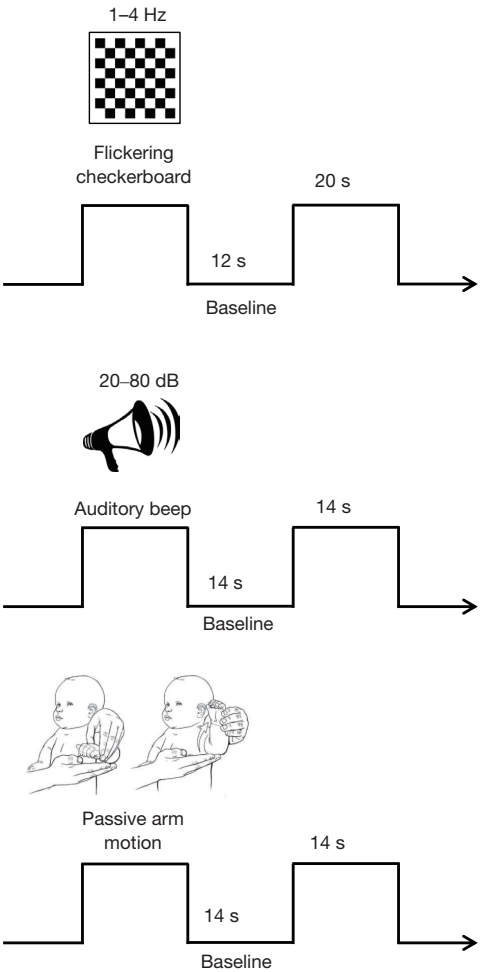

Figure 1 Experimental design.

in the anatomical predicted region of interest (ROI) for each stimulation. An expert neuroradiologist confirmed visually that identified ROIs corresponded to expected sensorimotor (and supplementary motor), primary auditory, and visual areas in neonates. To evaluate response profiles in identified ROIs, we extracted the BOLD signal within these clusters and averaged the signal across all stimulation blocks, excluding motion spike time points.

fNIRS data acquisition

The fNIRS signal was measured with the continuous wave Oxymon NIRS system (Artinis Medical Systems®, The Netherlands), with four emitters (with two light sources at 760 and 850 nm) and four detectors and sampling rate 25 Hz. A custom-made cap with optodes positioned in a diamond pattern (2–2.5 cm spacing) allowed to cover the scalp with four channels separately over the three regions of interest in the visual, auditory (left and right), or sensorimotor cortex (*Figure 2*). The cap was placed relative to three scalp landmarks (10–20 coordinate FPZ, right and left preauricular points), to match positions across participants. Acquisitions were accomplished during natural sleep, after feeding.

fNIRS data processing

Data processing was conducted with Homer2 (21) in MATLAB R2019a (MathWorks), following a standard approach to preprocessing and motion correction of infant fNIRS data (22,23). Raw light intensity was normalized and converted into optical density units. Motion was detected channel-by-channel (Homer2 function *hmrMotionArtifactByChannel*) by supra-threshold signal changes in amplitude and/or standard deviation within 0.5 s time-windows and points within 1 s of motion were marked as artifacts. A combination of spline interpolation (P=0.99) and wavelet filtering (IQR =1.5) was applied to correct motion artifacts, and artifact detection was applied again to reject from further analysis any epoch containing a remaining artifact between -2 s and the duration of each stimulation block. Resulting data were band-pass filtered between 0.01–1 Hz and converted to HbO, HbR, and total hemoglobin (HbT) concentrations changes, using a modified Beer-Lambert law (24) with specific differential path-length factors (DPF) adjusted for each wavelength and participants age (DPF_{760nm} =5.3 and DPF_{850nm} =4.2) (25).

fNIRS data analysis

Data were averaged channel-by-channel by condition (3 s prior to the start of the stimulation block + 10 s after) and baseline corrected to the epoch-specific pre-stimulus average. Our main analysis concerned whether functional brain activity (changes in HbO and anti-correlated HbR) was qualitatively observed in each channel.

Comparison between fMRI and fNIRS data

To optimize the comparison, high-frequency noisy time points in preprocessed fNIRS signal were identified and corrected using a Savitzky-Golay smoothing filtering procedure (26). Then, a frequency matching factor (TR_fMRI × frequency_fNIRS) was applied to the preprocessed and filtered fNIRS data to downsample its temporal

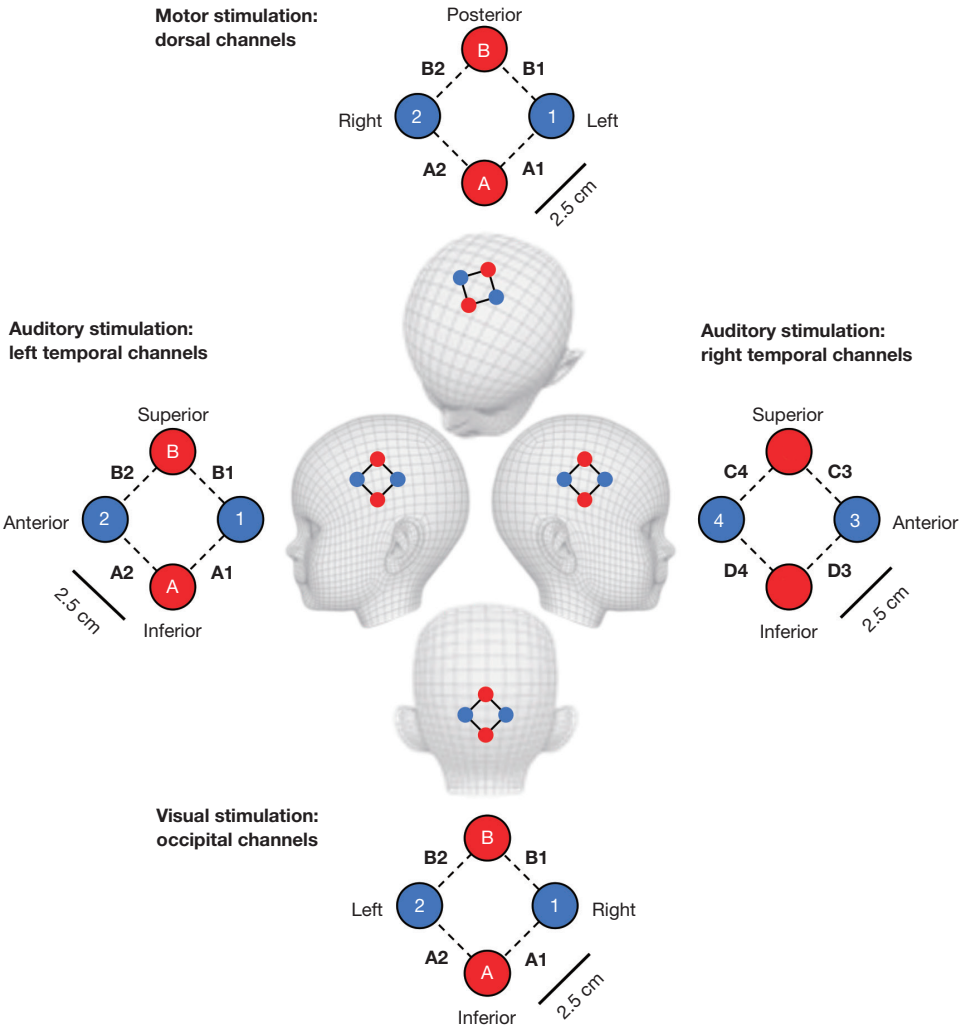

Figure 2 Schematic diagram of fNIRS optodes setup, showing the placement of the imaging arrays over the motor, temporal, and occipital cortex of a newborn, with top, lateral, and back views of the newborn's head. Red circles represent the light emitters and blue circles the light detectors. Each pair emitter/detector creates a channel (dotted lines), to which the measurements refer. fNIRS, functional near-infrared spectroscopy.

frequency to match the TR of the acquired fMRI data. This ensured equal and matching sampling points in response curves for both modalities.

Statistical analysis

Statistical analysis was performed using IBM-SPSS® v27, and statistical significance of 5% was considered. Measures of central tendency and dispersion were calculated for the quantitative variables, and absolute and relative frequencies for the qualitative variables. To compare quantitative variables the independent Student *t*-test or Mann-Whitney *U* test were performed as appropriate (normality verified using Kolmogorov-Smirnov tests). Pearson or Spearman correlations, as applicable, were used to assess the relationship between the sample points of the filtered and

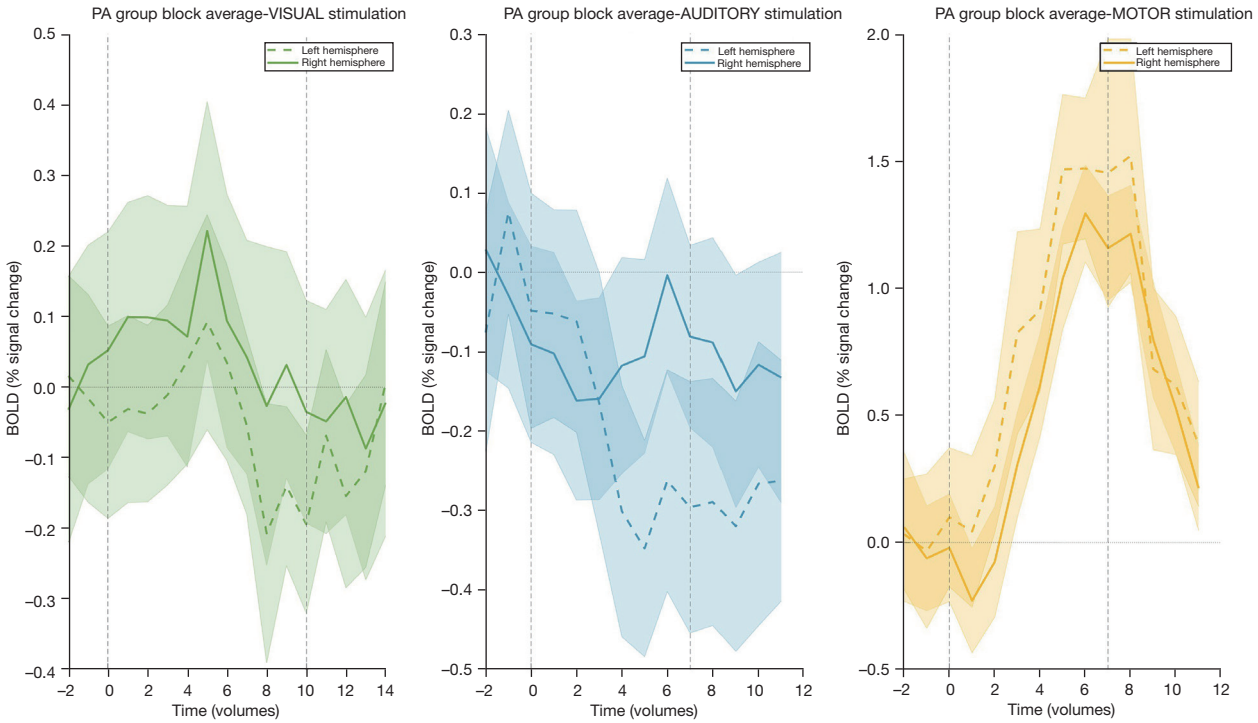

Figure 3 PA group block average BOLD mean response profiles. BOLD mean profile responses (% signal change) during visual, auditory, and sensorimotor (motor) stimulation in the respective regions of interest in each hemisphere (right: continuous line; left: dotted line). Note the lower variability of sensorimotor responses, possibly because neurovascular coupling maturation is fully achieved, and the asymmetric pattern in left and right brain hemispheres during auditory stimulation, which might reflect the well-recognized structural and functional asymmetries. BOLD, blood-oxygen-level-dependent; PA, perinatal asphyxia.

reduced fNIRS (HbO) and fMRI BOLD.

Results

Structural MRI

The results of the total MRI score, deep grey matter subscore, and cerebral white matter/cortex subscore can be observed in *Table 1*. Four newborns obtained the maximum punctuation, ranging from 15 to 26 in total score and 6 to 15 in the deep grey matter subscore. No lesions were observed in the newborn from the control group.

fMRI

In general, sensorimotor stimulation elicited the highest responses, which were BOLD signal increases (positive) relative to baseline in most cases. For visual stimulation, responses were essentially positive, with lower amplitude than the response to sensorimotor stimulation. An asymmetric pattern was observed for auditory stimulation with predominantly positive responses in the right hemisphere and negative (BOLD signal decreases) in the left. BOLD mean profile responses during visual, auditory, and sensorimotor stimulation in the respective ROI from PA group block average are provided in *Figure 3*. A table with a detailed, comprehensive description of the response patterns within identified ROI in each newborn, corresponding to different types of stimulation, is presented in Figure S1. There were no significant differences in fMRI BOLD signal in newborns concerning the type of sedation (Table S1).

fNIRS

Figure 4 presents the group average response profile (HbO and HbR), measured in each channel for each stimulation task for patients (PA) and controls and its comparison. In newborns with PA, the sensorimotor response was characterized by a slight increase in HbR (negative). The auditory and visual responses were characterized by increased

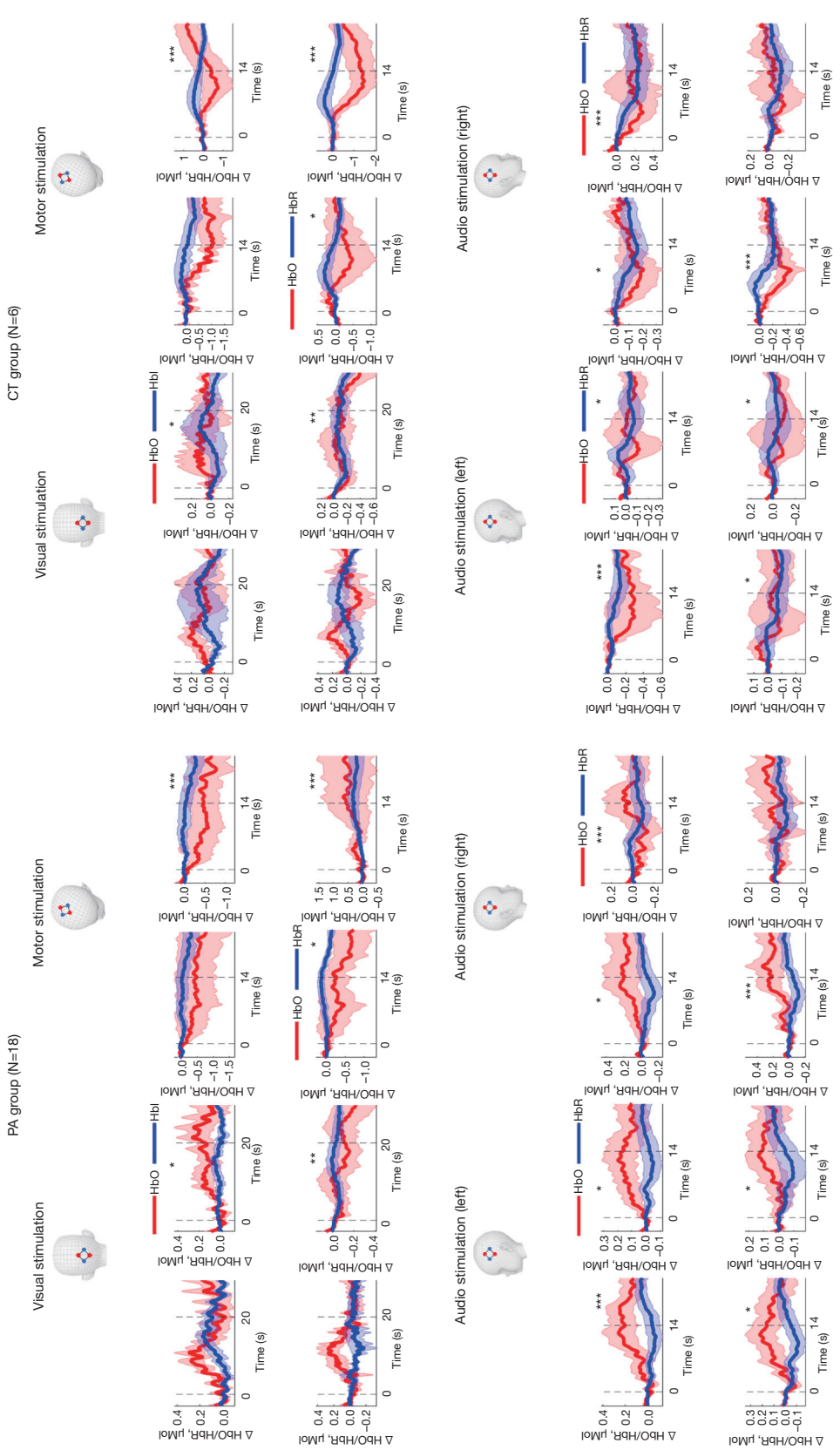

Figure 4 Summary of participants' fNIRS results. Each plot shows an average hemodynamic response to the corresponding stimulation type, visual, auditory (audio), and sensorimotor (motor) in PA and control groups. Each subset of 4 channels is presented in the same spatial location relative to each other, as in the scheme of the head on top of each subset (*Figure 2*). The dashed vertical lines indicate the beginning/end of the stimulation blocks. *, **, ***, for significative differences ($P<0.05$) between the newborns with PA and controls in the fNIRS sampling points filtered and downsampled of the HbO, HbR, or both, respectively (independent Student *t*-test or Mann-Whitney *U* test). Note that in at least two channels in all stimulation types, there were differences between newborns with PA and controls in the profile of HbO, HbR, or both; during auditory stimulation, this difference was more noticeable, being found in seven of the eight channels. PA, perinatal asphyxia; CT, control; HbO (red), oxyhemoglobin; HbR (blue), deoxyhemoglobin; fNIRS, functional near-infrared spectroscopy.

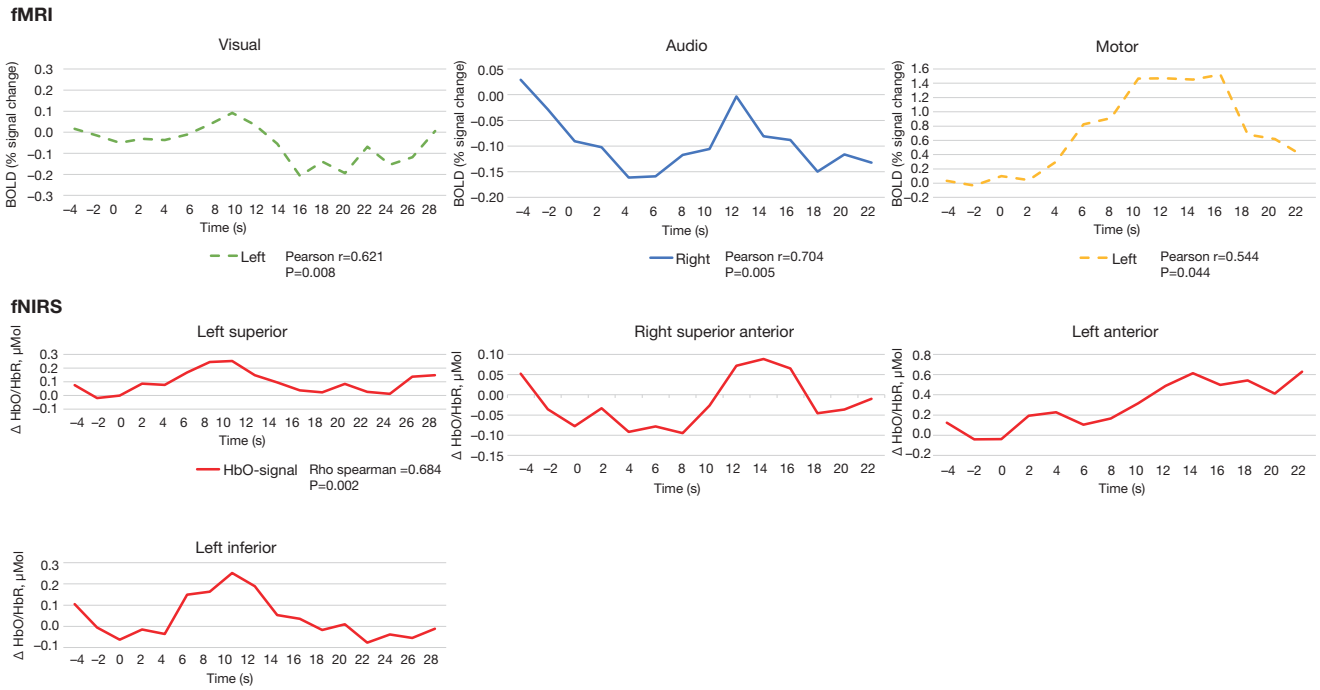

Figure 5 fMRI and fNIRS correlations in newborns with PA. Significative positive correlations by stimulus between sampling points of the fMRI positive BOLD signal by hemisphere and the filtered and reduced fNIRS HbO signal by channel. BOLD, blood-oxygen-level-dependent; fMRI, functional magnetic resonance imaging; fNIRS, functional near-infrared spectroscopy; audio, auditory; motor, sensorimotor; HbO, oxyhemoglobin.

HbO (positive).

Relationship between fMRI and fNIRS responses

The significative positive correlations by stimulus between sample points of the fMRI positive BOLD signal by hemisphere and the reduced and filtered fNIRS HbO signal by channel in newborns with PA can be observed in *Figure 5*. There was a positive correlation in all stimuli between signals from at least one channel of fNIRS and fMRI.

Discussion

As to our knowledge, this is the first study to investigate brain responses with fMRI and fNIRS in the same group of newborns. We observed polarized response profiles with both functional imaging techniques during multiple sensory stimulation with negative and positive shapes. Much debate has been going on the origin of this polarity/variability in newborn studies, particularly whether it is associated with physiological factors, namely the ongoing development of neurovascular coupling (NVC) and autoregulation mechanisms, and cerebral metabolic rate of oxygen ($CMRO_2$), extremely distinct from the adult brain (7,11,27). Our results, taking advantage of multiple sensory stimulations in the same acquisition session using optimized protocols (15,20), favor evidence of different NVC maturation levels in sensorimotor, visual, and auditory areas in newborns with PA. The much less variability in fMRI results during sensorimotor stimulation (essentially positive responses with higher amplitude), is corroborated by other fMRI reports, showing a lesser extent of variability in some newborn brain networks, possibly justified by genetic conditions (28) and that these areas are more active, temporally dynamic, and better connected than the primary auditory and visual areas (29). Accordingly, in recent years, a more robust activation pattern and a maturational trend of sequential functional responses with increasing postmenstrual age, similar to adult patterns, have been described using passive sensorimotor tasks (30,31). The NVC development trajectory may be related with functional hyperemia initiation improvement with increasing age, contributing to shifts in the CBF and $CMRO_2$ balance and influencing the direction of the signal in newborn functional

imaging studies (31-33).

In general, our fNIRS results are comparable to most studies that used auditory and visual paradigms similar to ours (6). However, most of them were performed in healthy newborns. Differences in HbO and HbR profiles were found in newborns with PA and controls, especially in auditory stimulation, which may be clinically helpful. Conversely, an fNIRS study in HIE newborns in the first three days of age observed an inverse pattern (34). It is important to underline that these results might be influenced by changes in CBF and cardiovascular function, that occur in the first days after PA (35). On the other hand, our functional imaging data were acquired in the second week of age, in a phase of clinical stability, circumventing the interference of the hemodynamic changes typical of PA in the first week of life. Furthermore, the difference in the number of newborns with PA and controls may have influenced our results. Thus, a direct comparison of results must be cautious. The sensorimotor response of a slight increase in HbR in newborns with PA maybe eventually justified by using a small probe scheme that precludes assessing broader cortical areas (6). Additional explanations for this inverse response include the vascular steal or vascular sharing effects, in which the regions adjacent to an activated region show a reduced regional CBF or vasoconstriction (33).

Comparison between fMRI and fNIRS

We identified positive correlations in newborns with PA between the fMRI BOLD signal and at least one fNIRS channel (HbO) in all stimuli: the strongest was in the auditory (r=0.704) and the weakest in the sensorimotor (r=0.544); in more fNIRS channels, in the visual. There are adult reports showing concordance between fMRI and fNIRS, and despite some controversy over which fNIRS measure best correlates with the fMRI BOLD signal, the HbO appears to have a strong correlation (36). However, there are also studies showing why they may deviate and may help to elucidate the correlation not observed in every fNIRS channel. One potential cause is related with different spatial resolution and partial volume effects (33,37). In our case, the well-known limited spatial and depth resolution of fNIRS may have been implicated, possibly associated with the cortical anatomic variability in newborns (8,36). Additionally, there are several other issues to consider that may have contributed to these result: while fMRI can measure the microcapillary bed, fNIRS poses more challenges in interpretation, since the signal related to activation can be originate from several vascular compartments (36); also, regarding analysis, methodology is better established in fMRI than in fNIRS. The GLM approach uses a predefined HRF, which can be different in newborns or in diverse cortical regions (38). Although we made an effort to adjust the HRF model for fMRI analysis according to literature in healthy infants, this might not hold true in (every case of) newborns with PA. In fNIRS literature, block averaging the mean concentration changes of HbO and HbR to extract activation patterns is the standard procedure (6). Some experts also recommend GLM for fNIRS analysis, but further optimization is required to be able to adjust the model of HRF in fNIRS analysis pipelines and software (38), as well as to optimize pre-processing strategies for infant fNIRS data (39). Perhaps less critical, unlike fMRI, the components of the fNIRS signal are more prone to be affected by changes in extracerebral compartment and systemic physiological parameters, making these possible confounders of neural activity (40). We did, however, account for this issue by employing low pass filtering and block averaging approaches. Moreover, the acquisitions of both functional imaging techniques were accomplished under different conditions, although on the same day: sedation was used to reduce head motion in fMRI, whereas fNIRS was performed during natural sleep. There are inconsistent statements concerning the influence of sedation on the CBF and the shape of the fMRI BOLD signal (8,20,41,42). Despite studies suggesting that its use did not weigh global CBF or the BOLD signal (20,42), we must state that using sedation to minimize motion artifacts and newborn distress may have influenced our results, possibly reducing signal amplitude.

Limitations

We acknowledge that a longer TE in fMRI could have increased image contrast and signal-to-noise ratio (43). Even with the suboptimal shorter TE used, we incurred the risk of missing significant signal changes rather than asserting spurious effects that would support erroneous conclusions. Furthermore, to enhance the detection of signal changes, we optimized the stimulation protocol and HRF model during data analysis (15,20). Besides other limitations exposed throughout the discussion, we must highlight that interpretation of functional activity, particularly in newborns with PA, should be cautious, since a normal pattern in healthy subjects is not yet fully

established (5,8). Furthermore, PA may disrupt NVC leading to abnormal hemodynamic parameters (44). This suggests that functional studies in newborns with PA might require a previous definition of HRF, achievable with specific event-related paradigms and deconvolution analysis. Despite the limitations and exploratory nature, this study has the strength of combining two promising and interesting functional imaging techniques in newborns with PA, boosting the use of fNIRS in neonatal intensive care units, especially taking into account the correlation observed between techniques and the possibility that fMRI may play a role in the prognosis of newborns with PA evoked in another study from our group (45).

Conclusions

Notably, we demonstrated that combined fMRI-fNIRS is feasible in this challenging context. The observation of variable/polarized functional imaging responses to multiple sensory stimulations in the same acquisition session can be explained by physiological/biological mechanisms, not artifacts. The relationship found may potentiate the clinical use of the fNIRS at the bedside as an alternative functional imaging tool to fMRI in newborns with PA.

Acknowledgments

We thank Robert J. Cooper from the Department of Medical Physics and Biomedical Engineering, University College London, United Kingdom, for his help with fNIRS data analysis. We also thank Sónia Afonso and Carlos Martins (from Institute of Nuclear Sciences Applied to Health (ICNAS), University of Coimbra, Coimbra, Portugal) for their support on MRI data acquisition and Ana Brett (from University Clinic of Pediatrics, Faculty of Medicine, University of Coimbra, Coimbra, Portugal) for the English revision. We are also very grateful to Barbara R. Correia (from the Quantitative Methods, Information and Management Systems Department, Coimbra Business School, Coimbra, Portugal) for the statistical support.
Funding: This work was supported by the Fundação para a Ciência e a Tecnologia, Lisboa/COMPETE 2020, Portugal (No. PTDC/DTP-PIC/6032/2014/POCI-01-0145-FEDER-016781).

Footnote

Reporting Checklist: The authors have completed the MDAR reporting checklist. Available at https://tp.amegroups.com/article/view/10.21037/tp-23-135/rc

Data Sharing Statement: Available at https://tp.amegroups.com/article/view/10.21037/tp-23-135/dss

Peer Review File: Available at https://tp.amegroups.com/article/view/10.21037/tp-23-135/prf

Conflicts of Interest: All authors have completed the ICMJE uniform disclosure form (available at https://tp.amegroups.com/article/view/10.21037/tp-23-135/coif). The authors have no conflicts of interest to declare.

Ethical Statement: The authors are accountable for all aspects of the work in ensuring that questions related to the accuracy or integrity of any part of the work are appropriately investigated and resolved. All procedures were carried out in accordance with the Declaration of Helsinki (as revised in 2013). The study was approved by the Ethics Committee of the Faculdade de Medicina da Universidade de Coimbra, Portugal (Reference CE-029-2014). Informed written consent was obtained from parents of all participants after a full verbal and written explanation of the study.

References

1. Marlow N, Shankaran S, Rogers EE, et al. Neurological and developmental outcomes following neonatal encephalopathy treated with therapeutic hypothermia. Semin Fetal Neonatal Med 2021;26:101274.
2. Mathew JL, Kaur N, Dsouza JM. Therapeutic hypothermia in neonatal hypoxic encephalopathy: A systematic review and meta-analysis. J Glob Health 2022;12:04030.
3. Wisnowski JL, Wintermark P, Bonifacio SL, et al. Neuroimaging in the term newborn with neonatal

encephalopathy. Semin Fetal Neonatal Med 2021;26:101304.
4. Lally PJ, Montaldo P, Oliveira V, et al. Magnetic resonance spectroscopy assessment of brain injury after moderate hypothermia in neonatal encephalopathy: a prospective multicentre cohort study. Lancet Neurol 2019;18:35-45.
5. Seghier ML, Hüppi PS. The role of functional magnetic resonance imaging in the study of brain development, injury, and recovery in the newborn. Semin Perinatol 2010;34:79-86.
6. de Roever I, Bale G, Mitra S, et al. Investigation of the Pattern of the Hemodynamic Response as Measured by Functional Near-Infrared Spectroscopy (fNIRS) Studies in Newborns, Less Than a Month Old: A Systematic Review. Front Hum Neurosci 2018;12:371.
7. Vasung L, Abaci Turk E, Ferradal SL, et al. Exploring early human brain development with structural and physiological neuroimaging. Neuroimage 2019;187:226-54.
8. Seghier ML, Lazeyras F, Huppi PS. Functional MRI of the newborn. Semin Fetal Neonatal Med 2006;11:479-88.
9. Yeung MK. An optical window into brain function in children and adolescents: A systematic review of functional near-infrared spectroscopy studies. Neuroimage 2021;227:117672.
10. Gilmore JH, Knickmeyer RC, Gao W. Imaging structural and functional brain development in early childhood. Nat Rev Neurosci 2018;19:123-37.
11. Kozberg M, Hillman E. Neurovascular coupling and energy metabolism in the developing brain. Prog Brain Res 2016;225:213-42.
12. Executive summary: Neonatal encephalopathy and neurologic outcome, second edition. Report of the American College of Obstetricians and Gynecologists' Task Force on Neonatal Encephalopathy. Obstet Gynecol 2014;123:896-901.
13. Shalak LF, Laptook AR, Velaphi SC, et al. Amplitude-integrated electroencephalography coupled with an early neurologic examination enhances prediction of term infants at risk for persistent encephalopathy. Pediatrics 2003;111:351-7.
14. Hellström-Westas L, Rosén I. Continuous brain-function monitoring: state of the art in clinical practice. Semin Fetal Neonatal Med 2006;11:503-11.
15. Cusack R, Wild C, Linke AC, et al. Optimizing stimulation and analysis protocols for neonatal fMRI. PLoS One 2015;10:e0120202.
16. Anderson AW, Marois R, Colson ER, et al. Neonatal auditory activation detected by functional magnetic resonance imaging. Magn Reson Imaging 2001;19:1-5.
17. Heep A, Scheef L, Jankowski J, et al. Functional magnetic resonance imaging of the sensorimotor system in preterm infants. Pediatrics 2009;123:294-300.
18. Weeke LC, Groenendaal F, Mudigonda K, et al. A Novel Magnetic Resonance Imaging Score Predicts Neurodevelopmental Outcome After Perinatal Asphyxia and Therapeutic Hypothermia. J Pediatr 2018;192:33-40.e2.
19. Friston KJ, Williams S, Howard R, et al. Movement-related effects in fMRI time-series. Magn Reson Med 1996;35:346-55.
20. Arichi T, Fagiolo G, Varela M, et al. Development of BOLD signal hemodynamic responses in the human brain. Neuroimage 2012;63:663-73.
21. Huppert TJ, Diamond SG, Franceschini MA, et al. HomER: a review of time-series analysis methods for near-infrared spectroscopy of the brain. Appl Opt 2009;48:D280-98.
22. Hyde DC, Simon CE, Ting F, et al. Functional Organization of the Temporal-Parietal Junction for Theory of Mind in Preverbal Infants: A Near-Infrared Spectroscopy Study. J Neurosci 2018;38:4264-74.
23. Di Lorenzo R, Pirazzoli L, Blasi A, et al. Recommendations for motion correction of infant fNIRS data applicable to multiple data sets and acquisition systems. Neuroimage 2019;200:511-27.
24. Strangman G, Culver JP, Thompson JH, et al. A quantitative comparison of simultaneous BOLD fMRI and NIRS recordings during functional brain activation. Neuroimage 2002;17:719-31.
25. Scholkmann F, Wolf M. General equation for the differential pathlength factor of the frontal human head depending on wavelength and age. J Biomed Opt 2013;18:105004.
26. Jahani S, Setarehdan SK, Boas DA, et al. Motion artifact detection and correction in functional near-infrared spectroscopy: a new hybrid method based on spline interpolation method and Savitzky-Golay filtering. Neurophotonics 2018;5:015003.
27. Takahashi T, Shirane R, Sato S, et al. Developmental changes of cerebral blood flow and oxygen metabolism in children. AJNR Am J Neuroradiol 1999;20:917-22.
28. Molloy MF, Saygin ZM. Individual variability in functional organization of the neonatal brain. Neuroimage 2022;253:119101.
29. Huang Z, Wang Q, Zhou S, et al. Exploring functional brain activity in neonates: A resting-state fMRI study. Dev

Cogn Neurosci 2020;45:100850.
30. Allievi AG, Arichi T, Tusor N, et al. Maturation of Sensori-Motor Functional Responses in the Preterm Brain. Cereb Cortex 2016;26:402-13.
31. Kozberg MG, Chen BR, DeLeo SE, et al. Resolving the transition from negative to positive blood oxygen level-dependent responses in the developing brain. Proc Natl Acad Sci U S A 2013;110:4380-5.
32. Kozberg MG, Ma Y, Shaik MA, et al. Rapid Postnatal Expansion of Neural Networks Occurs in an Environment of Altered Neurovascular and Neurometabolic Coupling. J Neurosci 2016;36:6704-17.
33. Moraschi M, DiNuzzo M, Giove F. On the origin of sustained negative BOLD response. J Neurophysiol 2012;108:2339-42.
34. Chen S, Sakatani K, Lichty W, et al. Auditory-evoked cerebral oxygenation changes in hypoxic-ischemic encephalopathy of newborn infants monitored by near infrared spectroscopy. Early Hum Dev 2002;67:113-21.
35. Hassell KJ, Ezzati M, Alonso-Alconada D, et al. New horizons for newborn brain protection: enhancing endogenous neuroprotection. Arch Dis Child Fetal Neonatal Ed 2015;100:F541-52.
36. Scarapicchia V, Brown C, Mayo C, et al. Functional Magnetic Resonance Imaging and Functional Near-Infrared Spectroscopy: Insights from Combined Recording Studies. Front Hum Neurosci 2017;11:419.
37. Abdalmalak A, Milej D, Cohen DJ, et al. Using fMRI to investigate the potential cause of inverse oxygenation reported in fNIRS studies of motor imagery. Neurosci Lett 2020;714:134607.
38. Pinti P, Scholkmann F, Hamilton A, et al. Current Status and Issues Regarding Pre-processing of fNIRS Neuroimaging Data: An Investigation of Diverse Signal Filtering Methods Within a General Linear Model Framework. Front Hum Neurosci 2018;12:505.
39. Gemignani J, Gervain J. Comparing different pre-processing routines for infant fNIRS data. Dev Cogn Neurosci 2021;48:100943.
40. Erdoğan SB, Yücel MA, Akın A. Analysis of task-evoked systemic interference in fNIRS measurements: insights from fMRI. Neuroimage 2014;87:490-504.
41. Slupe AM, Kirsch JR. Effects of anesthesia on cerebral blood flow, metabolism, and neuroprotection. J Cereb Blood Flow Metab 2018;38:2192-208.
42. Yamamoto AK, Magerkurth J, Mancini L, et al. Acquisition of sensorimotor fMRI under general anaesthesia: Assessment of feasibility, the BOLD response and clinical utility. Neuroimage Clin 2019;23:101923.
43. Goksan S, Hartley C, Hurley SA, et al. Optimal echo time for functional MRI of the infant brain identified in response to noxious stimulation. Magn Reson Med 2017;78:625-31.
44. Bell AH, Miller SL, Castillo-Melendez M, et al. The Neurovascular Unit: Effects of Brain Insults During the Perinatal Period. Front Neurosci 2019;13:1452.
45. Pinto CR, Duarte JV, Marques C, et al. The role of early functional neuroimaging in predicting neurodevelopmental outcomes in neonatal encephalopathy. Eur J Pediatr 2023;182:1191-200.

Cite this article as: Pinto CR, Duarte JV, Dinis A, Duarte IC, Castelhano J, Pinto J, Oliveira G, Castelo-Branco M. Functional neuroimaging of responses to multiple sensory stimulations in newborns with perinatal asphyxia. Transl Pediatr 2023;12(9):1646-1658. doi: 10.21037/tp-23-135

Supplementary

	fMRI responses																											
	BOLD (% signal change)						SEM BOLD (% signal change)						t-value						p-value						number of voxels					
	VISUAL		AUDITORY		SENSORIMOTOR		VISUAL		AUDITORY		SENSORIMOTOR		VISUAL		AUDITORY		SENSORIMOTOR		VISUAL		AUDITORY		SENSORIMOTOR		VISUAL		AUDITORY		SENSORIMOTOR	
PA01		0.251	-0.211	-0.23	0.951	0.622		0.053	0.064	0.065	0.249	0.123		4.75	-3.306	-3.561	3.827	5.068		0.000004	0.00132	0.000467	0.000214	0.000002		76	56	46	57	37
PA02		-0.366	-0.309	-0.328	0.941			0.094	0.077	0.067	0.274			-3.894	-4.003	-4.933	3.433			0.000136	0.000088	0.000002	0.00085			54	100	198	26	
PA03		-0.345				-0.395		0.09				0.096		-3.854				-4.111		0.000159				0.000072		34				86
PA04	0.147	-0.214	-0.136				0.032	0.078	0.025				4.549	-2.766	-5.442				0.000009	0.006219	0.0000001				58	98	181			
PA05		0.161	-0.134			0.302		0.039	0.03			0.059		4.133	-4.432			5.162		0.000053	0.000015			0.000001		41	107			15
PA06	0.464	0.515			-0.32		0.147	0.149			0.122		3.164	3.45			-2.624		0.001807	0.000688			0.009933		62	59		114		
PA07	-0.384	-0.401	-0.202				0.119	0.136	0.029				-3.214	-2.944	-6.867				0.001579	0.003719	0.0000001				93	87	219			
PA08		0.327	-0.233	0.166				0.111	0.071	0.046				2.942	-3.286	3.629				0.00367	0.001208	0.000365				86	116	106		
PA09	0.176	0.155				0.244	0.063	0.053				0.034	2.788	2.903				7.068	0.005831	0.004121				0.0000001	81	42				204
PA10	-0.236			0.252		0.77	0.071			0.041		0.136	-3.313			6.154		5.658	0.001095			0.0000001		0.0000001	99			81		32
PA11	-0.131	0.171		0.176	0.883	1.127	0.026	0.029		0.032	0.114	0.185	-5.105	5.811		5.417	7.727	6.102	0.000001	0.0000001		0.0000001	0.0000001	0.0000001	123	496		92	306	68
PA12	0.135		0.22	0.159	1.459	2.385	0.038		0.058	0.029	0.174	0.329	3.554		3.816	5.567	8.403	7.24	0.000478		0.000182	0.0000001	0.0000001	0.0000001	22		41	71	71	97
PA13			-0.154	-0.161		1.436			0.044	0.028		0.249			-3.523	-5.745		5.754			0.000524	0.0000001		0.0000001			29	311		107
PA14	0.137		0.166	0.14	0.884	0.716	0.032		0.039	0.037	0.137	0.087	4.245		4.296	3.733	6.457	8.245	0.000034		0.000027	0.000245	0.0000001	0.0000001	14		26	13	357	426
PA15		-0.191	-0.237	0.193		0.207		0.034	0.052	0.04		0.053		-5.606	-4.558	4.855		3.887		0.0000001	0.000009	0.000002		0.000158		107	95	50		16
PA16	-0.176	0.131				0.649	0.04	0.034				0.104	-4.384	3.856				6.24	0.000019	0.000157				0.0000001	42	65				91
PA17			-0.381	-0.333	-0.867				0.124	0.102	0.201				-3.059	-3.269	-4.319				0.002506	0.001262	0.00003				53	109	70	
PA18	-0.14			-0.169		-0.499	0.029			0.027		0.092	-4.765			-6.212		-5.402	0.000004			0.0000001		0.0000001	43			59		23
CT01		-0.144	.096			0.586		0.023	0.02			0.178		-6.321	4.769			3.296		0.0000001	0.000003			0.001259		77	91			24

Figure S1 Comprehensive description of fMRI response patterns. Comprehensive description of the fMRI response patterns during visual, auditory, and sensorimotor stimulation (beta values, standard error, t values, P values, and number of voxels of the clusters) per participant and brain hemisphere. PA, perinatal asphyxia participants; CT, control participant; fMRI, functional magnetic resonance imaging; BOLD, blood-oxygen-level-dependent; SEM, standard error of the mean.

Table S1 fMRI BOLD responses by type of sedation in participants with PA

fMRI BOLD responses (% signal change) per stimulus and hemisphere	Sedation type		P
	Midazolam (N=7)	Propofol (N=11)	
Visual left, mean ± SD	0.757±0.428	−0.0336±0.175	0.563
Visual right, mean ± SD	−0.057±0.363	−0.119±0.189	0.303
Auditory left, median (IQR)	−0.202 (−0.26 to 0.135)	−0.193 (−0.273 to 0.195)	1.0
Auditory right, median (IQR)	−0.279 (−0.328 to −0.279)	0.159 (−0.165 to 0.184)	0.145
Sensorimotor left, mean ± SD	0.524±0.731	0.52±1.001	0.928
Sensorimotor right, mean ± SD	0.176±0.52	0.782±0.821	0.266

fMRI, functional magnetic resonance imaging; BOLD, blood-oxygen-level-dependent; PA, perinatal asphyxia; N, number; SD, standard deviation; IQR, interquartile range. Retrieved with permission from Pinto CR, Duarte JV, Marques C, Vicente IN, Paiva C, Eloi J, et al. The role of early functional neuroimaging in predicting neurodevelopmental outcomes in neonatal encephalopathy. Eur J Pediatr. 2023;182(3):1191-200. Copyright license at https://creativecommons.org/licenses/by/4.0/.

https://dx.doi.org/10.21037/tp-23-135